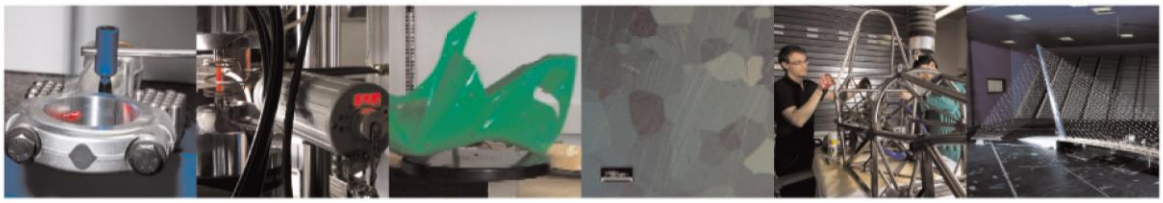

Shape distortion reduction method for abrasive water jet (AWJ) cutting

Hlaváč, Libor M.; Hlaváčová, Irena M.; Arleo, Francesco; Viganò, Francesco; Annoni, Massimiliano Pietro Giovanni; Geryk, Vladan

This is a post-peer-review, pre-copyedit version of an article published in PRECISION ENGINEERING. The final authenticated version is available online at: http://dx.doi.org/10.1016/j.precisioneng.2018.04.003

Shape distortion reduction method for abrasive water jet (AWJ) cutting

L.M. Hlaváč, I.M. Hlaváčová, F. Arleo, F. Viganò, M. Annoni, V. Geryk

Abstract

The aim of this study is to test a theoretical model for calculating abrasive water jet (AWJ) cutting parameters in order to reduce the shape deformation in curved cutting trajectories. Experimental results were produced using commercial AWJ machines. Despite the limitations of these commercial AWJ machines in terms of both software and hardware, the comparison of calculated and experimental results showed a sufficient correspondence between the theoretical and experimental data sets, with the difference lying within the range of measurement uncertainty. The difference between theoretical and experimental results is up to 2.5 %, similarly to the combined measurement uncertainty. The maximum deviations of the measured values from the calculated averages are up to 0.2 mm and the measuring device uncertainty is up to 0.1 mm. A method aimed at reducing the shape distortion caused by AWJ in curved geometric features is suggested and tested. It was unambiguously demonstrated that the jet markedly reduces the shape deformation in curved geometric features when it is tilted according to the proposed method. Such an error compensation procedure can be already applied on commercial machines.

Keywords

Abrasive water jet (AWJ); Cutting; Declination angle; Taper; Distortion; Compensation

Nomenclature:

a_m	average size of material structural units [m]
C_A	coefficient for adjusting jet power with respect to variations in abrasive content below and above the saturation level [-]
C_Q	coefficient enabling calculation of the traverse speed ensuring achievement of desired cut wall quality (based on limit traverse speed) [-]
d_0	water jet diameter [m]
d_a	abrasive water jet diameter [m]
D_I	inlet diameter of the column sample cut by AWJ [mm]
D_O	outlet diameter of the column sample cut by AWJ [mm]
D_{OB}	basic outlet diameter of the column sample cut by AWJ (deformation caused only by trailback) [mm]
D_{Ie}	experimentally determined inlet diameter of the column sample cut by AWJ [mm]
D_{It}	inlet diameter of the column sample cut by AWJ calculated from theory [mm]
D_{Oe}	experimentally determined outlet diameter of the column sample cut by AWJ [mm]
D_{Ot}	outlet diameter of the column sample cut by AWJ calculated from theory [mm]
ΔD_N	percentage difference of the average inlet and outlet diameters of the column sample cut by non-tilted AWJ (ΔD_{N20} for outlet declination angle 20°) [%]
ΔD_T	percentage difference of the average inlet and outlet diameters of the column sample cut by tilted AWJ (ΔD_{T20} for compensated declination angle 20°) [%]
H	material thickness [m]
K	material resistance to abrasive (e.g. hardness) [-]
L	stand-off distance [m]

p_j pressure determined from density and speed of abrasive jet [Pa]
S_P coefficient of particle integrity (ratio of number of intact particles to total number of particles) [-]
t interaction time [s]
v_P traverse speed [m·s^{-1}]
v_{P20} traverse speed calculated for outlet declination angle 20° [m·s^{-1}]
v_{Plim} limit traverse speed calculated for cutting material of thickness H [m·s^{-1}]
v_{Pmin} minimum traverse speed – correction for stopped movement – it is determined from average abrasive particle size [m·s^{-1}]
v_{PQ} traverse speed ensuring achievement of desired cut wall quality throughout the thickness H of the material [m·s^{-1}]
α_e coefficient of jet speed loss in the interaction process with the material [-]
θ positive value of angle determined at the depth h between the tangent to the striation curve and the jet axis at the point of impact [°]
θ_{lim} absolute value of angle determined at the depth h_{lim} between the tangent to the striation curve and the jet axis at the point of impact [°]
ξ_j coefficient of attenuation of abrasive jet between focusing tube outlet and material surface [m^{-1}]
ρ_j density of abrasive jet (conversion to homogeneous liquid) [kg·m^{-3}]
ρ_m density of machined material [kg·m^{-3}]
σ tensile strength (or compressive strength) of processed material [Pa]

1. Introduction

Abrasive water jets (AWJ) can cut materials with high accuracy and quality, provided that suitable parameters are set for the process. AWJ can also be applied for milling [1 - 3], turning [4 - 6], grinding [7], polishing [8] and complex machining [9]. However, cutting of shapes from plate-type materials remains the most frequent application up to now. Although this method can achieve very good standards of quality, there is still space for improvement. The study presented in this paper can be used to improve the AWJ cutting quality, thus generating economic benefits.

Cutting of materials by AWJ has been studied by Hashish [10], Zeng and Kim [11], Paul et al. [12, 13], who prepared first models for calculation of the depth of cut in material. Later on many other researchers [14 - 23] studied various aspects of the cutting process both analytically and experimentally. Hlaváč prepared theoretical model based on physical laws of conservation [14], Momber explained stress-strain phenomena during erosion process of the AWJ [15], Vikram and Babu [16], Chen et al. [17], Deam et al. [18] and Orbanic and Junkar [19] prepared models for prediction of the surface topography, namely formation of striations during cutting process. Caydas and Hascalik [20] studied the surface roughness, Srinivasu et al. [21] focused their research on machining of the silicon carbide ceramics, Srinivas and Babu [22] prepared an analytical model for AWJ cutting of ductile materials and Thomas [23] studied the formation of cavities on surfaces cut by AWJ. One of the specific approaches to the explanation of several phenomena occurring during AWJ cutting of materials was taken by Hlaváč [24]. His theory is based on the laws of conservation of energy and momentum [14] and on a geometric analysis of phenomena caused by AWJ on cut walls [25]. The theoretical description of the depth of AWJ penetration into material is the topic of the paper [14]. The extension of this model by description of the declination angle

dependence on either depth of AWJ penetration to material or on the limit traverse speed for selected material thickness were presented namely in [24]. Hlaváč et al. [25] introduced the theoretical description of product distortion caused by AWJ trailback and method of application of this model.

The deflected jet shape when passing through the material has been studied also by several other authors [17, 18, 19, 21, 22]. Their conclusions can be combined with the findings described in [24], especially the equations for calculating the jet delay and the related declination angle. Most of the published studies focus on the characteristic traces left by the AWJ process on the material surface, namely striations and roughness (see e.g. [16, 19, 20, 23, 26]). Nevertheless, Hlaváč considers the declination angle being the one of the sensitive output variables reflecting the AWJ parameters setting and the material properties [24]. His method for determining the declination angle and examining its dependency on the cutting head traverse speed is described mainly in publications [24, 25]. He correlated his results also with material properties [27] and found the equations for calculation of taper dependence on the traverse speed [28, 29], because the model presented in [30] was specific for ceramics. The present paper focuses primarily on comparing the results of his previously presented theoretical equations used to predict the shape variance in an AWJ-cut sample with experimental results obtained when "column" samples are cut from plates of various thickness using commercial AWJ machines enabling "tilted-jet" cutting. During experimental works it appeared that some of the automatic compensations implemented to software of commercial machines could not be switched off by operator. Searching for the machine enabling experimental set up according to theoretical requirements took several years. This contribution presents experimental results and their correlation with Hlaváč's theory, as well as gradual way to the final solution of the problem. This appeared to be preparation of a special device ensuring correct conditions of the required set-up for demonstration of the trailback impact on product distortion. Some of the experimental results were performed without compensation of the taper. In these cases the taper has been calculated from model presented in past [28, 29] and its value was subtracted from experimental values to obtain pure influence of trailback.

2. Theoretical basis

The theoretical basis for this study comes from a model derived for limit cutting parameters [24]. This study is based primarily on Eq. (1) [25], which enables the limit traverse speed v_{Plim} to be calculated for a given material thickness. The coefficient α_e defined by Eq. (2) was derived from the law of momentum conservation at the micro-level (grain of abrasive – grain of material); it determines the effectiveness of the disintegration process and its relation to selected material properties and several characteristics of the liquid jet [25, 27].

$$v_{Plim} = \left[\frac{C_A S_P \pi d_0 \sqrt{2\rho_j p_j^3 e^{-5\xi_j L}} \left(1-\alpha_e^2\right)}{8H\left(p_j \rho_j \alpha_e^2 e^{-2\xi_j L} + \sigma\rho_j\right)} \right]^{\frac{2}{3}} - v_{Pmin} \tag{1}$$

$$\alpha_e = 1 - \frac{\sqrt{2p_j^3}\,Kt}{8\sqrt{\rho_j}\,a_m \sigma} \tag{2}$$

For the purpose of determining the traverse speed v_{PQ}, which allows achieving the desired walls quality, the basic relation for determining the limit traverse speed was complemented by the coefficient C_Q (see [24, 25]). The speed v_{PQ} is determined by the Eq. (3).

$$v_{PQ} = C_Q v_{Plim} \tag{3}$$

The dependency of the declination angle on either traverse speed v_{Plim} (alternatively v_{PQ}) or the material thickness [24] can be used to determine the jet delay, which causes workpiece deformations (see line segment BC in Fig. 1). The declination angle is calculated at a selected traverse speed from the relation shown in Eq. (4), which was introduced for this purpose in [25]:

$$\vartheta = \vartheta_{lim} \left(\frac{v_P}{v_{Plim}} \right)^{\frac{3}{2}} \tag{4}$$

A suitable jet tilting at the point of impact when moving along a curved trajectory should significantly compensate for the shape deformation of the sample caused by the jet delay (the trailback). On the basis of many experiments [24, 25, 27], the optimum tilt angle was determined to be one half of the expected declination angle. The aim of the study presented in this paper was to verify the findings presented in previous theoretical works by Hlaváč [24, 25, 27] using commercial equipment with programmable cutting head tilting.

The following process was selected in order to carry out this verification. For a selected declination angle, the appropriate traverse speed v_{PQ} for the given material was calculated based on Eq. (4), derived from the above-mentioned model [25]. Cuts were performed on plane-parallel metal plates along circular trajectories using calculated traverse speeds with both non-tilted (Fig. 1a) and tilted (Fig. 1b) jets. When using the tilted jet, the plane λ was required to be tangential to the circle described by the intersection of the jet axis and the workpiece surface at every point on the trajectory (see Fig. 1b, where λ is determined by the jet axis and the perpendicular to the workpiece surface at the point of jet impact). Fig. 1b shows the position of the plane λ when cutting a “column” sample using a tilted jet. The expected jet trajectory when penetrating the material is marked as a solid line and the expected deformation of the column sample after cutting (in accordance with the theoretical conclusions presented in [25]) is marked with a dotted line. The diameters on the inlet (D_I) and the outlet (D_O) bases of "columns" cut from plane parallel material are included into Fig. 1 as they are the studied parameters compared with each other and with respective results calculated from the presented theoretical base.

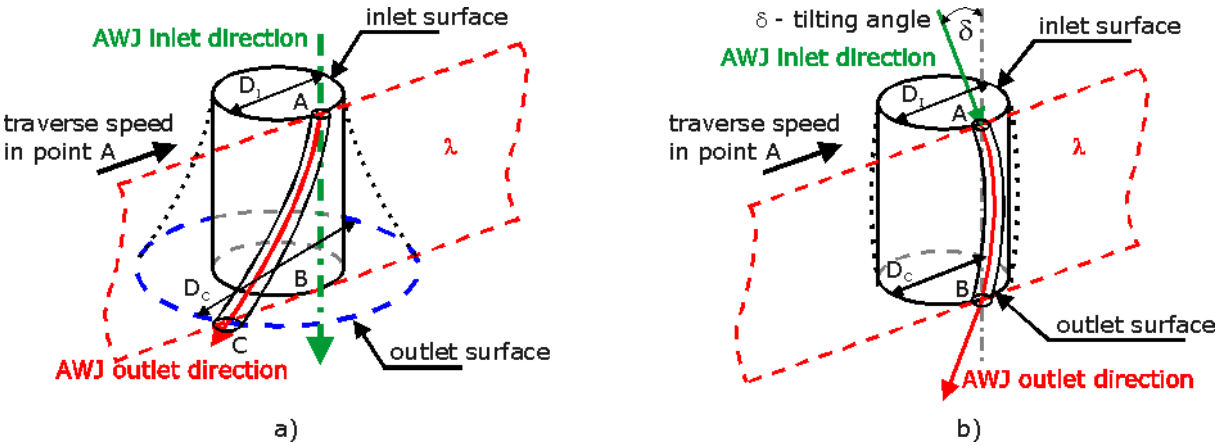

Fig. 1. a) Column sample distortion: Plane λ is determined by points ABC; A is the intersection of the jet axis with the inlet surface, B is the intersection of the jet entry axis with the outlet surface, and C is the intersection of the momentary axis of the curved cutting jet with the outlet surface (the solid red line marks the trajectory of the jet penetrating the material and lying in plane λ, the dotted line marks the resulting sample shape), D_I and D_O are the diameters of "column" product on the inlet and outlet side of plate material.

b) Compensation of column sample distortion: Plane λ is determined by the jet axis (the green arrow) and the perpendicular to the workpiece surface at the point of impact, and it is tangential to the side surface of the cut column sample. The red line marks the trajectory of the jet penetrating the material and lying in plane λ.

The preparation and evaluation of the experiments are based on the following two assumptions presented also in [24]:

- the offset between the actual jet axis and the kerf forming face centre line is constant and equal to $d_a/2$ and both the lines lay on λ plane (i.e. jet is considered to be non-converging or diverging in the direction of the traverse speed, only in the direction perpendicular to the cut walls);
- the shape of the striations produced on the cut wall is identical to the shape of the kerf forming face centre line.

These theoretical considerations form the basis for determining the cut wall quality and for calculating the declination angle at the given depth in material [24, 25]. They also enable the calculation of the suitable jet tilt angle that compensates the workpiece shape deviations at a given traverse speed and for a given material thickness. The jet tilt angle can be altered in a smooth and gradual way to match the changing traverse speed during cutting: this way it is possible to considerably reduce occurrences of overcutting and undercutting at the beginning and at the end of the cut trajectory, as well as in case of sudden changes in the cut direction (edges of angular samples).

3. Experiments and Results

The experiments aimed at verifying or correcting the theoretical assumptions were carried out at the laboratories of the VŠB-Technical University of Ostrava (Czech Republic) and the Department of Mechanical Engineering - Politecnico di Milano (Italy). The equipment in each case consisted of a pump and a CNC handling system. The respective equipment was: table PTV WJ1020-1Z-EKO and pump Flow HSQ 5X in Ostrava; table CMS-TECNOCUT IDRO 1740

and pump Flow 9XV-S as the machine 1 in Milano; table INTERMAC PRIMUS 322 and pump BHDT ECOTRON 4037 as the machine 2 in Milano. The selected parameters at the individual workplaces are presented in Table 1.

Tab. 1. Values of pre-set parameters of cutting

Variable (unit)	Ostrava (laboratory)	Milano (machine 1)	Milano (machine 2)
Pressure in pump (MPa)	380	350	350
Water jet diameter (mm)	0.254	0.254	0.330
Focusing tube diameter (mm)	1.02	1.02	1.02
Focusing tube length (mm)	76	76	76
Abrasive mass flow (g/min)	250	300	300
Mean abrasive grain size*) (mm)	0.25	0.25	0.25
Abrasive type**)	AG	AG	AG
Stand-off distance (mm)	2	3	3

*) Measurements of AG garnet 80 mesh was performed in certified Laboratory of Powdery Materials at the VŠB – Technical University of Ostrava on the machine Mastersizer 2000 and confirmed on the Fritsch Analysette 22 MicroTec plus.
**) Abrasive type is almandine Australian garnet (AG)

3.1 The first step of the experimental approach

The first experiments were carried out in Ostrava on metal samples summarized in Table 2 in 2012. The cut shape was a cylindrical “column” with “cutting diameter” 10 mm that is sufficiently small to measure differences between the inlet and the outlet side with satisfactory accuracy. “Cutting diameter” means diameter of the nominal circle drawn by the intersection of the jet axis with the material surface without considering any jet radius offset. Thus the jet dimension is not considered in this study since the only interesting value to be studied is the difference between the inlet D_I and the outlet D_O "column" diameters for non-compensated and compensated declination angle. All the samples measurements were carried out using a contact digital device (Lobster® Vernier calliper). Also other contact devices were tested; the Hitec digital micrometre and the device for measuring cylindricity Zeiss Prismo Navigator coordinate measuring machine. The tested optical method was based on transformation of the column base area to the respective circle diameter. The photos from the Nikon D300 camera or the INFINITY2-3C camera on NOVEX Holland microscope were analysed using i-Solution software. The difference between contact and non-contact methods was within the range of uncertainties. The maximum deviations of measured values from the calculated averages were up to 0.2 mm and the uncertainty of the measuring device was up to 0.1 mm. The combined uncertainty of measurement was up to 2.5 % for the smallest measured column diameters (8.9 mm) for both types of tested methods. Therefore, the simplest and fastest method has been selected. Measuring device Zeiss Prismo Navigator is not usable for all samples, because the measuring tip can be broken when the unevenness of the measured surface is too sharp and large, as on the bottom part of tested samples of hard steels. Finally, the fastest and more flexible device, the Vernier calliper, has been used for all measurements.

First experiments in Ostrava were made only with the jet axis angle 0°, i.e. for the jet perpendicular impact on the surface, because the equipment did not allow jet tilting. Traverse speeds were calculated for the declination angle 20° at the bottom edge. This

declination angle corresponds with medium cutting quality, which is considered the most economical solution for most applications. However, at this angle the jet delay causes visible sample deformations, overcuts and undercuts. The respective cutting speed to achieve the necessary declination angle (see Table 2) was calculated from Eq. 5 (modified Eq. 4) in the first series of experiments for each material separately. The calculation was based on previous declination angles measurements. The relevant limit declination angle is 45° for v_{Plim} when cutting thin samples (up to 20 mm). Table 2 shows the sample thickness H, the calculated cutting speed v_{P20} and the theoretical and experimental values for both the inlet and the outlet diameters in perpendicular (non-tilted) cutting, determined from measurements carried out at a traverse speed corresponding with a declination angle of 20° at the outlet point. The percentage differences between calculated (D_{It} or D_{Ot}) and measured (D_{Ie} or D_{Oe}) values for both the inlet and the outlet diameters (ΔD_I and ΔD_O) were added for better understanding the theoretical model precision.

$$v_P = v_{Plim}\left(\frac{\vartheta}{\vartheta_{lim}}\right)^{\frac{2}{3}} \tag{5}$$

The first set of experiments was performed on nine metal samples (see Table 2). The set of 9 column samples has been cut without tilting and with pre-set diameter of jet axis trajectory 10 mm. The heights of the "columns" correspond with thicknesses of the steel plates used for sample preparation and diameters of the top and bottom bases were calculated from theory and measured on samples (see Table 2). These samples were used for correlation of experimental and theoretical results of inlet and outlet diameters.

Tab. 2. Ostrava – perpendicular cuts: Theory and experiment. Steel plate thicknesses H, limit traverse speed v_{Plim}, traverse speed v_{P20} calculated for declination angle 20°, theoretical inlet D_{It} and outlet D_{Ot} diameters, experimental inlet D_{Ie} and outlet D_{Oe} diameters, percentage differences ΔD_I and ΔD_O of the average theoretical and experimental values determined for the inlet and outlet diameters.

Material type	H	v_{Plim}	v_{P20}	D_{It} *)	D_{Ie}	D_{Ot}	D_{Oe}	ΔD_I	ΔD_O
WNR norm (DIN norm)	mm	mm/min	mm/min	mm	mm	mm	mm	%	%
1.057 (St 52-3)	10	250	146	8.98	8.96	9.41	9.45	0.22	0.42
1.0503 (C 45)	10	200	116	8.96	9.00	9.52	9.63	0.44	1.14
1.7131 (16 MnCr 5)	10	220	128	8.96	8.92	9.42	9.64	0.45	2.28
1.7225 (42 CrMo 4)	10	180	105	8.96	8.97	9.48	9.64	0.11	1.66
1.4541 (X6 CrNiTi 18 10)	10	200	116	8.96	8.98	9.39	9.36	0.22	0.32
1.2436 (X210 CrW 12)	10	160	93	8.94	8.92	9.64	9.82	0.22	1.83
1.0038 (RSt 37-2)	10	300	175	8.97	8.98	9.50	9.60	0.11	1.04
1.0038 (RSt 37-2)	15	200	116	8.96	8.99	9.62	9.87	0.33	2.53
1.0038 (RSt 37-2)	20	140	82	8.96	8.98	9.98	10.22	0.22	2.35

*) Theoretical inlet diameter is calculated from the circle diameter set on the cutting machine and the diameter of the abrasive water jet calculated from the formula for jet divergence considering stand-off distance measured on machine.

3.2 The second step of the experimental approach

Since the equipment in Ostrava did not allow cutting with tilted jet, it was decided to perform the experiments in Milano, where the tilted cutting configuration was allowed. The experiments performed in 2013 were carried out on machine 1. Cutting samples with the jet axis perpendicular to the surface plane presented no problem. Conversely, some issues appeared when cutting in tilted configuration. According to the presented theory, the point of jet axis impact on the material surface should move along a curved trajectory. At the same time, the jet axis should always be oriented tangent to the planned side wall of the cut column (as it was explained in the theoretical part – Fig. 1b) and tilted 10° from the perpendicular to the material surface to compensate declination angle of 20° at the bottom outlet (corresponding to experiments without tilting). The implementation of the original plan encountered some key problems. The experiments which best met the requirements enabling comparison with data from theoretical calculations were performed on a 5-axis machine 1. However, these experiments were not entirely free from problems and a certain change of the planned experimental procedure was needed. The traverse speed was automatically decreased by software control. Therefore, it was necessary to correct it in manual mode. Moreover, the software automatically started with lower traverse speed and before the end of cut decreased the traverse speed. The same metal plates, like in the first step, were used for this part of the experiment, but 18 "columns" were cut this time: 9 samples were cut with jet perpendicular to the surface of metal plate and the next 9 samples were cut with tilting angle 10°. The results from both the experiments are summarized in Table 3.

Tab. 3. Milano – cutting on machine 1, first set of samples: Inlet D_I and outlet D_O diameters of "columns" measured on samples prepared at the identical speed v_{P20} intended (calculated) for non-tilted jets producing declination angle 20° and tilted jets with 10° eliminating distortion effects caused by trailback. The percentage differences between the inlet and the outlet column bases are compared for non-tilted ΔD_{N20} and tilted ΔD_{T20} jets.

			non-tilted		tilted		difference	
Material type	H	v_{P20}	D_I	D_O	D_I	D_O	ΔD_{N20}	ΔD_{T20}
WNR norm (DIN norm)	mm	mm/min	mm	mm	mm	mm	%	%
1.057 (St 52-3)	10	146	8.77	9.53	9.14	9.76	8.7	6.8
1.0503 (C 45)	10	116	8.80	9.50	9.13	9.57	7.9	4.8
1.7131 (16 MnCr 5)	10	128	8.81	9.56	9.16	9.79	8.6	6.9
1.7225 (42 CrMo 4)	10	105	8.79	9.40	9.08	9.59	6.9	5.6
1.4541 (X6 CrNiTi 18 10)	10	116	8.80	9.43	9.03	9.52	7.2	5.5
1.2436 (X210 CrW 12)	10	93	8.80	9.51	9.08	9.61	8.1	5.9
1.0038 (RSt 37-2)	10	175	8.87	9.68	9.10	9.70	8.7	4.2
1.0038 (RSt 37-2)	15	116	8.83	10.12	9.02	9.77	13.6	5.9
1.0038 (RSt 37-2)	20	82	8.84	10.58	9.10	10.12	17.9	9.6

3.3 The third step of the experimental approach

In 2014 it was decided to try another experimental approach at the machine 1 in Milano. Only steel samples with similar composition and identical thickness were tested using uniform traverse speed for anticipated declination angle 20° (calculated from Hlaváč's model). The cuts were performed with jet axis perpendicular to the steel plate and with tilting angle 10° that should compensate deformation caused by trailback. All 14 samples (7 samples cut by perpendicular jet, 7 samples cut with tilting jet) were cut from steel plates 20 mm thick, so they all have the same heights. The results of measured top and bottom diameters are summarized in Table 4. The traverse speed is identical for all selected samples (steels with very similar characteristics). This experiment has shown that tilting of the jet axis proposed from Hlaváč's theoretical works [24, 25] improves the outlet diameter of the "column" product substantially.

Tab. 4. Milano – cutting on machine 1, second set of samples: "Column" samples of stainless and alloyed steels made by non-tilted and tilted jets from 20 mm thick plates: the pre-set traverse speed was 60 mm/min, the inlet D_I and the outlet D_O diameters were measured and the respective percentage differences for non-tilted ΔD_N and tilted ΔD_T jets were determined.

			non-tilted		tilted		difference	
Material type	H	v_{P20}	D_I	D_O	D_I	D_O	ΔD_N	ΔD_T
WNR norm (DIN norm)	mm	mm/min	mm	mm	mm	mm	%	%
1.4034 (X46 Cr 13)	20	60	8.69	11.85	8.95	10.31	30.8	14.1
1.4404 (X2 CrNiMo 17 13 2)	20	60	8.68	11.10	8.93	10.20	24.5	13.2
1.4541 (X6 CrNiTi 18 10)	20	60	8.64	10.92	8.92	10.21	23.4	13.5
1.4713 (X10 CrAl 7)	20	60	8.70	11.20	8.95	9.95	25.1	10.6
1.4762 (X10 CrAl 24)	20	60	8.70	11.30	8.87	10.20	26.0	14.0
1.4828 (X15 CrNiSi 20 12)	20	60	8.64	10.97	8.84	10.24	23.8	14.7
1.4845 (X12 CrNi 25 21)	20	60	8.69	11.09	8.88	11.10	24.2	12.8

3.4 The fourth step of the experimental approach

Since the experiment needed for verifying the benefits of tilted-jet cutting according to the proposals published in [25] requires compliance with the geometry shown in Fig. 1b, some more experimental works were performed. One of the problems was that the jet axis needed to be situated on a plane remaining constantly tangential to the outer surface of the cut "column" sample throughout the entire rotation. Moreover, this rotational movement needed to be entirely smooth. Additionally, it would be ideal if the angle proportionally increases or decreases with the changing traverse speed. In this case, the angle may change from zero for a zero speed at the beginning, up to the required value for the set traverse speed, and then back to zero when stopped at the end. Another requirement was that the traverse speed during the cutting operation of the whole column should remain constant. No one of these requirements could be fully met in previous steps of the research. Therefore, the machine 2 in Milano has been selected for experiments in 2015. However, the commercial equipment usually superposes its specific slow-down algorithms, thus not

offering such possibilities for completely controlling this operation without complications. For that reason, approximate experiments were carried out with slightly changed conditions. First of all, it was also necessary to add a linear part of the cutting path that enabled to stabilize the traverse speed (Fig. 2). Next, the centreline trajectory diameter was changed to 12 mm, because some experiments indicated improper machine behaviour (see Fig. 3). Therefore, the results could have been potentially distorted. The final set-up of experiment can be described as follows. The cut starts with piercing of material in point 1. Jet is perpendicular to the metal plate. Jet starts moving along the linear part of the trajectory and the traverse speed stabilises. Then the trajectory changes to circular part and the first (left, marked P) "column" is cut with perpendicular jet at constant traverse speed. After finishing the circle jet decelerates on the linear part of trajectory and stops in point 2 on straight line between columns. The cutting head tilts at that point to the angle 10° as it is impossible to do it in the required manner during cutting. Then jet starts to accelerate again on the straight line. After reaching stable traverse speed the second circle with tilted head is performed cutting the "column" by tilted jet (marked T). The final linear part to the point 3 is again for deceleration. However, the small "automatic" decrease of the traverse speeds introduced by machine in circular parts of the trajectories regarding the pre-set values needed to be corrected manually, because it was not possible to eliminate it by program (opposite to the acceleration and deceleration during starting and ending part of cutting eliminated introducing linear parts of cut outside "column" outline). Twenty six "column" samples from 13 metal plates were cut. All column samples are 10 mm high. Thirteen columns were cut with perpendicular jet and the next thirteen ones with tilted jet. The respective sizes of top and bottom bases, as well as other results from this research period are summarized in Table 5, columns are presented in Fig. 4.

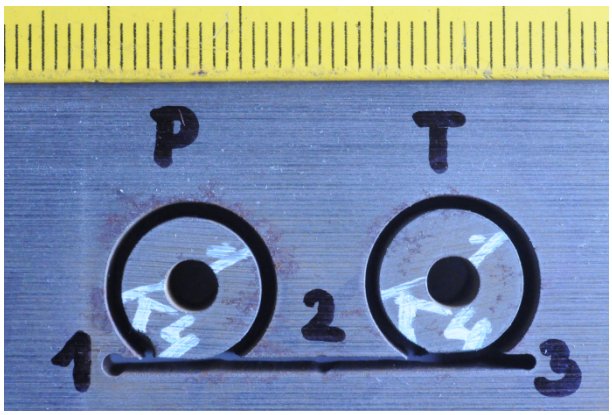

Fig. 2. Changed settings of the experiments in Milano 2015: Trajectory used for eliminating the pre-sets issues of the machine used for experiments – see explanation in text (P – part of cutting made by perpendicular jet, T – part of cutting made by tilted jet); experimental material 1.2436 (X210 CrW 12)

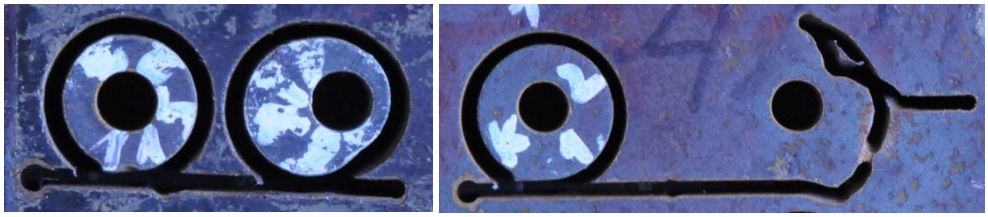

Fig. 3. Problems occurring during cutting of "column" samples with diameter 10 mm on machine 2 (the internal holes are for fixing tool) - the diameter was increased to 12 mm in view of the problems.

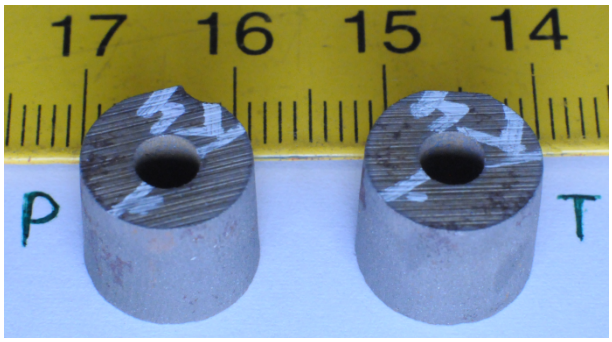

Fig. 4. View of the columns cut from experimental material - steel 1.2436 (X210 CrW 12) in Milano on machine 2

Tab. 5. Milano – cutting on machine 2, third set of samples: Inlet D_I and outlet D_O diameters of "columns" measured on samples prepared at the identical speed v_{P20} intended for non-tilted jets producing declination angle 20° and tilted jets with 10° inclination eliminating distortion effects caused by the trailback. The focuser centreline diameter to cut the column base was set to 12 mm (no jet radius offset considered). The percentage differences between the inlet and the outlet column bases are compared for non-tilted ΔD_{N20} and tilted ΔD_{T20} jets.

			non-tilted		tilted		difference	
Material type	H	v_{P20}	D_I	D_O	D_I	D_O	ΔD_{N20}	ΔD_{T20}
WNR norm (DIN norm)	mm	mm/min	mm	mm	mm	mm	%	%
1.057 (St 52-3)	10	193	10.76	11.38	11.18	11.58	5.7	3.6
1.0503 (C 45)	10	153	10.82	11.48	11.13	11.60	6.1	4.2
1.7131 (16 MnCr 5)	10	169	10.82	11.43	11.22	11.59	5.7	3.4
1.7225 (42 CrMo 4)	10	139	10.82	11.39	11.21	11.56	5.3	3.1
1.4541 (X6 CrNiTi 18 10)	10	153	10.82	11.41	11.22	11.58	5.5	3.3
1.2436 (X210 CrW 12)	10	123	10.82	11.50	11.17	11.59	6.3	3.8
3.2315 (AlMgSi1Mn)	10	577	10.75	11.36	11.16	11.51	5.7	3.2
3.1325 (AlCu4MgSi)	10	585	10.78	11.43	11.13	11.54	6.0	3.6
3.4345 (AlZn5Mg3Cu)	10	553	10.85	11.41	11.19	11.53	5.2	3.0
2.0060 (E-Cu57)	10	292	10.90	11.42	11.23	11.51	4.8	2.5
HARDOX500 PLATE	10	103	10.81	11.28	11.18	11.54	4.3	3.2
2.0402 (CuZn40Pb2)	10	290	10.79	11.32	11.20	11.51	4.9	2.8
1.0038 (RSt 37-2)	10	186	10.77	11.37	11.11	11.52	5.6	3.7

3.5 The fifth step of the experimental approach

To eliminate problems with the machine software, it was decided to interchange the relative movement of the sample and the cutting device. A special device has been designed and developed (Fig. 5). This device consists of a rotating support carrying the material fixed on it. The device needs a specific adjustment procedure to achieve the desired effect (cutting of one circle of desired diameter with tilted jet), but its application for the sample preparation presents the best possible opportunity to fulfil presumptions matching exactly the design of the compensation test drawn in Fig. 1b. Adjustment consists of setting the point of intersection for either the perpendicular or the tilted jet to the rotational device axis intersection with cut material surface. The problem is, that rotational axis is in a free space (because this is the area of cutting) and it is necessary to identify its intersection with material surface first of all. Then it is possible to set the jet so that its axis intersects material surface in this point. Subsequently it is possible to move the jet from this position to the new one in the distance of desired radius of cut "column" plus radius of the jet. The cut is performed so that the rotating device is put into movement simultaneously with moving the

jet from its position to the distance matching radius of the cut "column". The rotational movement is stopped after one revolution. The jet is switched off simultaneously.

Fig. 5. Special device for rotating the samples: testing device for the trailback compensation (declination angle influence) on circular samples, pictures a) and b) show two positions during device operation; jet is tilted 10°from the perpendicular to the sample surface

Finally, more accurate experiments verifying theoretical models were performed on the special device presented in Fig. 5 enabling the sample rotation while maintaining a constant jet tilt angle at the table. Experiments with this special device were performed in Ostrava in 2016 and the centreline trajectory on the material inlet surface was set to 10 mm. Fourteen samples (seven samples with perpendicular jet and seven samples with tilted jet) all 10 mm high were cut in this stage. An example of cut columns is presented in Fig. 6. Results of these experiments are presented in Table 6. The inlet D_I and outlet D_O diameters of "columns" were measured on samples prepared at the identical speed v_{P20} producing an outlet declination angle of 20° for non-tilted jets and eliminating distortion effects caused by trailback with a 10° jet tilting. The percentage differences between the inlet and the outlet column bases are. Experimental parameters and factors correspond to the column "Ostrava" in Table 1. Simultaneously, the calculations of the respective geometric parameters characterizing the samples were calculated from the reported theoretical equations by Hlaváč and presented in brief form in the theoretical part of this article. The respective trailback and taper were calculated according to equations presented in previous publications [25, 28, 29]. The necessary additional corrections based on these calculations are summarized in Table 7, presenting the sample deformation without any compensation, the respective trailback and taper calculated from presented theory and comparison of such results with experimental ones. Table 8 shows the state with tilted jet, when the trailback is compensated by jet tilting and it is necessary to determine the taper – the values calculated from presented theory are submitted and the total theoretical compensation result is summarized.

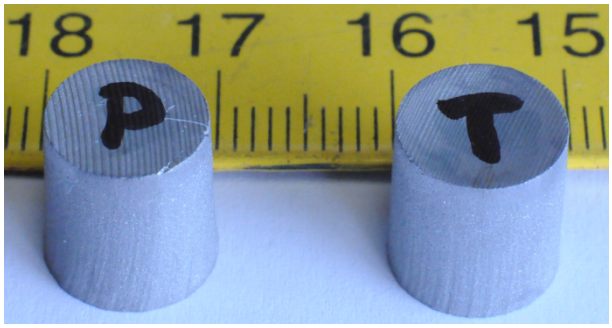

Fig. 6. An example of columns cut on special device for rotating the samples: experimental material 1.4541 (X6 CrNiTi 18 10)

Tab. 6. Ostrava – experiments with rotating sample: The fourth set of results was carried out using special device (Fig. 2): inlet D_I and outlet D_O diameters of "columns" are reported. Identical speed v_{P20} applied produces an outlet declination angle of 20° for non-tilted jet and eliminates distortion effects caused by trailback with a 10° jet tilting. The percentage differences between the inlet and the outlet column bases are compared (ΔD_{N20} for non-tilted, ΔD_{T20} for tilted).

			non-tilted		tilted		difference	
Material type	H	v_{P20}	D_I	D_O	D_I	D_O	ΔD_{N20}	ΔD_{T20}
WNR norm (DIN norm)	mm	mm/min	mm	mm	mm	mm	%	%
1.057 (St 52-3)	10	146	8.95	9.95	9.33	9.73	10.6	4.2
1.0503 (C 45)	10	116	8.96	9.88	9.33	9.66	9.8	3.5
1.7131 (16 MnCr 5)	10	128	8.95	9.98	9.32	9.73	10.8	4.3
1.7225 (42 CrMo 4)	10	105	8.95	9.75	9.32	9.63	8.6	3.4
1.4541 (X6 CrNiTi 18 10)	10	116	8.94	9.77	9.31	9.62	8.8	3.2
1.2436 (X210 CrW 12)	10	93	8.95	9.82	9.34	9.66	9.3	3.5
HARDOX 500 PLATE	10	79	8.96	9.63	9.32	9.61	7.1	3.1

Percentage differences presented in Tables 7 and 8 are differences between respective diameters D_I and D_O determined from the experiments (Table 6) and the ones calculated from the theoretical model for non-tilted (Table 7) or tilted (Table 8) jets. The calculated trailback is zero for tilted jet, because according to the presumption, the 10° tilting angle should compensate the trailback caused by the traverse speeds v_{P20}.

Tab. 7. Ostrava – theoretical determination of deformation parameters for non-tilted jet: Trailback, taper and total deformation results calculated by the presented theory and percentage differences of total calculated results from experimental ones presented in Table 6 (left column - inlet diameter, right column - outlet diameter).

				deformation					
Material type	H	v_{P20}	D_I	trailback	taper	D_{OB}	D_O	differences	
WNR norm (DIN norm)	mm	mm/min	mm	mm	mm	mm	mm	%	
1.057 (St 52-3)	10	146	8.96	1.45	0.35	9.54	9.89	0.05	0.60
1.0503 (C 45)	10	116	8.96	1.46	0.36	9.54	9.90	0.00	0.20
1.7131 (16 MnCr 5)	10	128	8.96	1.48	0.36	9.56	9.92	0.12	0.56
1.7225 (42 CrMo 4)	10	105	8.96	1.47	0.36	9.56	9.92	0.16	1.71
1.4541 (X6 CrNiTi 18 10)	10	116	8.96	1.47	0.36	9.55	9.92	0.19	1.49
1.2436 (X210 CrW 12)	10	93	8.96	1.45	0.36	9.54	9.90	0.13	0.85
HARDOX 500 PLATE	10	79	8.96	1.45	0.35	9.54	9.89	0.00	2.68

Tab. 8. Ostrava – theoretical determination of deformation parameters for tilted jet: Trailback, taper and the total compensation results calculated by the presented theory for tilting angle 10° and percentage differences of total calculated results from the experimental ones presented in Table 6 (left column - inlet diameter, right column - outlet diameter). Column D_{OB} is removed because $D_{OB} = D_I$ due to supposed compensation.

				compensation				
Material type	H	v_{P20}	D_I	trailback	taper	D_O	differences	
WNR norm (DIN norm)	mm	mm/min	mm	mm	mm	mm	%	
1.057 (St 52-3)	10	146	9.33	± 0	0.35	9.68	0.01	0.48
1.0503 (C 45)	10	116	9.30	± 0	0.36	9.66	0.28	0.06
1.7131 (16 MnCr 5)	10	128	9.29	± 0	0.36	9.65	0.36	0.84
1.7225 (42 CrMo 4)	10	105	9.30	± 0	0.36	9.66	0.22	0.24
1.4541 (X6 CrNiTi 18 10)	10	116	9.28	± 0	0.36	9.64	0.32	0.25
1.2436 (X210 CrW 12)	10	93	9.31	± 0	0.36	9.67	0.29	0.03
HARDOX 500 PLATE	10	79	9.33	± 0	0.35	9.68	0.14	0.74

4. Discussion

Primarily it needs to be stated that none of the handling systems, available for the experimental work, enabled to achieve a full compensation according to the theoretical presumptions. It is caused by the fact that commercial machines are equipped with their own control software. Programming of the desired motions should need to modify such software, thus requiring an expensive and time-consuming task, not justified by this testing activity. Furthermore, the use of commercial devices and software demonstrated how far the compensation approach could go without substantially modifying the conventional

machine. The verification is based on application of the trailback compensation and calculation of the respective taper compensation.

The equipment with five degrees of freedom enabled the jet to be tilted and to maintain a constant angle of tilting throughout the circular cutting movement, which is a necessary condition for the comparison between the theory and the experimental data as shown in Fig. 1b. Nevertheless, the traverse speed was changed by the machine software. The real traverse speed was not correlating with the pre-set value, because it was reduced when the abrasive water jet was turned on. Therefore an ultimate correction was introduced, increasing the traverse speed 1.32 times to compensate the reduction introduced by the software. However, the analysed experiments were performed with traverse speeds not differing more than 2 % from the pre-set values (checked by measurement of the real traverse speed provided by the machines internal measuring tools). As it is clear from the experimental results summarized in Tables 2 through 7, it can be stated that tilting the jet axis (cutting head) works well. Results in Table 2 show very good agreement between theory and experimental data. Tables 3 through 6 indicate that a cutting head tilting brings substantial improvement even when not all presumptions are met. The most sensible improvement can be seen in the case of thicker samples (Table 4) and when the traverse speed is stabilized (Table 5). The experiments on the special device (Table 6) proved the same improvement. The agreement between the theoretical and experimental data is very good and the jet tilting compensates considerably for the shape imperfections caused by the jet delay (trailback) when cutting along curved trajectories. This can be seen also in Fig. 7, showing pictures of top and bottom of plates with "columns" cut by a non-tilted jet (A) and a tilted jet (B). The figures also clearly show the stepped motion of the jet at the outlet ascribable to the intrinsic cutting mechanism, causing waviness.

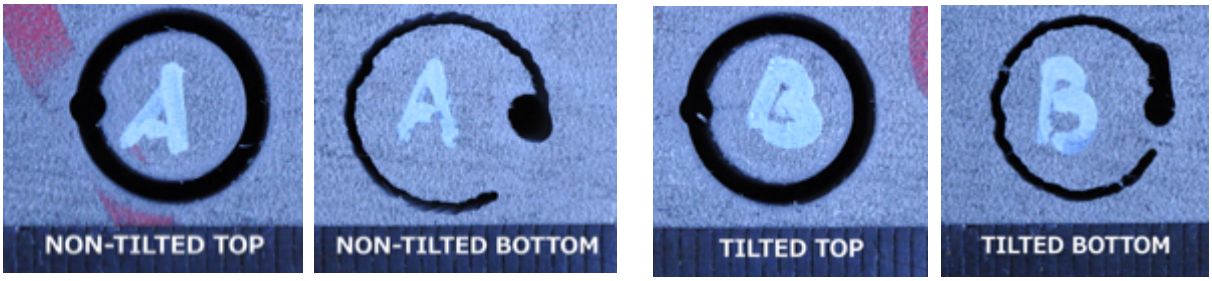

Fig. 7. Inlet and outlet edges of circular cuts: Circle diameter 10 mm (Table 4) made in 20 mm thick steel plate 1.4845 (X12 CrNi 25 21): A – non-tilted jet, B – tilted jet. The traverse speed was 60 mm/min and other cutting parameters are identical with those in Table 1, column Milano (machine 1)

Calculations of trailback, taper and respective diameters of samples in the case of non-tilted (Table 7) and tilted (Table 8) jets show conclusively that trailback is eliminated by jet tilting in the plane tangent to the curved surface of the kerf wall. The residual difference can be reasonably ascribed to the taper effect (calculated from equations presented in [28, 29]). The differences can be caused by the fact that an average value of constants has been used in the equations, because the relationship between the material structure and these constants is not fully described yet.

In view of the uncertainties of both the sample preparation procedure and the measurement of sample dimensions, it was impossible to determine the real amount of the

taper effect (as described in [28-30]). The device for sample rotation, which enabled cutting with an exactly defined jet tilting, can yield data facilitating the calculation of “pure” trailback and “pure” taper deformations. Measurements and calculations show very good correlation of data from both the procedures. However, the magnitude of both the trailback and the taper depends also on the abrasive mixing process and abrasive quality [31, 32]. Some of those studies were already presented in [33, 34]. A very important role can be played also by the properties describing the material behaviour [27] as strength, toughness, hardness, density, etc. Therefore, during the next period of research, it is necessary to focus also on mixing process analyses, with simulations and mathematical analyses of all related processes. Experiments on one type of material in various states (like in [27]) should be also very beneficial; therefore, they are also planned for the future. Up-to-date results, presented in Table 7 and Table 8, show a good correlation between calculated and experimental data reported in Table 6 (when the special device eliminating uncertainties and irregular motion of commercial machines was applied). Therefore, one of the next research programmes will be focused on the precision issue of both the commercial cutting devices and the special laboratory devices.

5. Conclusions

Experiments focusing on abrasive water jet cutting of column-shaped samples demonstrated that the presented theoretical model is a good predictor of traverse speed for selected declination angles, and that it can therefore be expected that the model will be suitable for determining the optimum tilt angle for a given momentary traverse speed. It was found that commercial AWJ machines have several hardware- and software-related limitations, and therefore the presented theoretical model can only be fully applied to compensate for AWJ-caused shape deformations if the software of the machinery can be programmed according to the model. Nevertheless, regardless of the current software and hardware limitations of machinery, it was unambiguously demonstrated that tilted-jet cutting according to the proposed model considerably reduces shape deformation of samples in the curved parts of the cutting trajectory. Finally, the application of a special non-commercial device definitely proved that proper jet tilting in the plane tangent to the curved surface of the kerf wall eliminates the deformation caused by the trailback.

Acknowledgements

This paper was prepared with the support of the Project No. LO1203 "Regional Materials Science and Technology Centre - Feasibility Program" and project No. SP2017/44, both funded by Ministry of Education, Youth and Sports of the Czech Republic.
The Authors are grateful to Giacomo Didoni, for his support in managing the devices in Politecnico di Milano Laboratories.

References

[1] Fowler, G., Shipway, P.H., Pashby, I.R., 2005. Abrasive water-jet controlled depth milling of Ti6Al4V alloy - an investigation of the role of jet-workpiece traverse speed and abrasive grit size on the characteristics of the milled material. Journal of Materials Processing Technology, 161(3), 407-414

[2] Alberdi, A., Rivero, A., Lopez de Lacalle, L.N., Etxeberria, I., Suarez, A., 2010. Effect of process parameter on the kerf geometry in abrasive water jet milling. International Journal of Advanced Manufacturing Technology, 51(5–8), 467–480

[3] Rabani, A., Madariaga, J., Bouvier, C., Axinte, D., 2016. An approach for using iterative learning for controlling the jet penetration depth in abrasive waterjet milling. Journal of Manufacturing Processes, 22, 99-107

[4] Hlaváč, L.M., Palička, P., 2006. Testing of parameters for turning by abrasive water jet. In Water Jetting, BHR Group, United Kingdom, p. 123-128. ISBN 1-85598-080-0

[5] Zohourkari, I., Zohoor, M., Annoni, M., 2014. Investigation of the Effects of Machining Parameters on Material Removal Rate in Abrasive Waterjet Turning. Advances in Mechanical Engineering, Article Number 624203

[6] Hlaváček, P., Carach, J., Hloch, S., Vasilko, K., Klichová, D., Klich, J., Lehocká, D., 2015. Sandstone Turning by Abrasive Waterjet, Rock Mechanics and Rock Engineering, 48(6), 2489-2493

[7] Liang, Z., Xie, B., Liao, S., Zhou, J., 2015. Concentration degree prediction of AWJ grinding effectiveness based on turbulence characteristics and the improved ANFIS. International Journal of Advanced Manufacturing Technology, 80(5-8), 887-905

[8] Che, C.L., Huang, C.Z., Wang, J., Zhu, H.T., Li, Q.L., 2008. Theoretical model of surface roughness for polishing super hard materials with Abrasive Waterjet. Advances in Machining and Manufacturing Technology IX, Key Engineering Materials, 375-376, 465-469

[9] Kong, MC; Srinivasu, D; Axinte, D; Voice, W; McGourlay, J; Hon, B, 2013. On geometrical accuracy and integrity of surfaces in multi-mode abrasive waterjet machining of NiTi shape memory alloys. CIRP Annals-Manufacturing Technology, 62(1), 555-558

[10] Hashish, M., 1989. A Model for Abrasive - Waterjet (AWJ) Machining. Transactions of the ASME, 111(2), 154-162

[11] Zeng, J., Kim, T.J., 1996. An erosion model of polycrystalline ceramics in abrasive waterjet cutting. Wear, 193, 207-217

[12] Paul, S., Hoogstrate, A.M., van Luttervelt, C.A. and Kals, H.J.J., 1998. Analytical and Experimental Modeling of Abrasive Water Jet Cutting of Ductile Materials. Journal of Materials Processing Technology, 73, 189-199

[13] Paul, S., Hoogstrate, A.M., van Luttervelt, C.A. and Kals, H.J.J., 1998. Analytical Modeling of the Total Depth of Cut in Abrasive Water Jet Machining of Polycrystalline Brittle Materials. Journal of Materials Processing Technology, 73, 206-212

[14] Hlaváč, L.M., 1998. JETCUT - software for prediction of high-energy waterjet efficiency. In: Louis, H. (Ed.), 14th International Conference on Jetting Technology, BHR Group Limited, Prof. Eng. Pub. Ltd., Bury St Edmunds & London, Brugge, Belgium, pp. 25-37

[15] Momber, A.W., 2001. Stress-strain relation for water-driven particle erosion of quasi-brittle materials. Theoretical and Applied Fracture Mechanics, 35(1), 19-37

[16] Vikram, G., Babu, N.R., 2002. Modelling and Analysis of Abrasive Water Jet Cut Surface Topography. International Journal of Machine Tools and Technology, 42(12), 1345-1354

[17] Chen, F.L., Wang, J., Lemma, E., Siores, E., 2003. Striation formation mechanisms on the jet cutting surface. Journal of Materials Processing Technology, 141(2), 213-218

[18] Deam, R.T., Lemma E., Ahmed, D.H., 2004. Modelling of the abrasive water jet cutting process. Wear, 257(9-10), 877-891

[19] Orbanic, H., Junkar, M., 2008. Analysis of striation formation mechanism in abrasive water jet cutting. Wear, 265(5-6), 821-830

[20] Caydas, U., Hascalik, A., 2008. A study on surface roughness in abrasive waterjet machining process using artificial neural networks and regression analysis method. Journal of Materials Processing Technology, 202(1-3), 574-582

[21] Srinivasu, D.S., Axinte, D.A., Shipway, P.H., Folkes, J., 2009. Influence of kinematic operating parameters on kerf geometry in abrasive waterjet machining of silicon carbide ceramics. International Journal of Machine Tools & Manufacture, 49(14), 1077-1088

[22] Srinivas, S., Babu, N.R., 2009. An analytical model for predicting depth of cut in abrasive waterjet cutting of ductile materials considering the deflection of jet in lateral direction. International Journal of Abrasive Technology, 2(3), 259-278

[23] Thomas, D.J., 2013. Characterisation of aggregate notch cavity formation properties on abrasive waterjet cut surfaces. Journal of Manufacturing Processes, 15(3), 355-363

[24] Hlaváč, L.M., 2009. Investigation of the Abrasive Water Jet Trajectory Curvature inside the Kerf. Journal of Materials Processing Technology, 209(8), 4154-4161

[25] Hlaváč, L.M., Strnadel, B., Kaličinský, J., Gembalová, L., 2012. The model of product distortion in AWJ cutting. International Journal of Advanced Manufacturing Technology, 62(1-4), 157-166

[26] Fabian, S., Servátka, M., 2009. New access at improvement of samples surface relief representation accuracy cut with AWJ technology with binding on increase of experiments evaluation objectivity and effectiveness. In: Fabian, S. (Ed.) Scientific Papers operation and diagnostics of machines and production systems operational states (Vol. 2), 1st edn. RAM-Verlag, Germany, pp. 9-15

[27] Strnadel, B., Hlaváč, L.M., Gembalová, L., 2013. Effect of steel structure on the declination angle in AWJ cutting. International Journal of Machine Tools & Manufacture, 64, 12-19

[28] Hlaváč, L.M., Hlaváčová, I.M., Gembalová, L., Jonšta, P.: Experimental investigation of depth dependent kerf width in abrasive water jet cutting. In: 20th International Conference on Water Jetting, F.H. Trieb (ed.), BHR Group, United Kingdom, 2010, p. 459-467

[29] Hlaváč, L.M., Hlaváčová, I.M., Geryk, V., Plančár, Š.: Investigation of the taper of kerfs cut in steels by AWJ. International Journal of Advanced Manufacturing Technology, 77(9-12), 2015, 1811-1818.

[30] Shanmugam, D.K., Wang, J., Liu, H., 2008. Minimisation of kerf tapers in abrasive waterjet machining of alumina ceramics using a compensation technique. International Journal of Machine Tools & Manufacture, 48, 1527-1534

[31] Salokyová, Š. 2016. Measurement and analysis of mass flow and feed speed impact on technological head vibrations during cutting abrasion resistant steels with abrasive water jet technology. Key Engineering Materials, 669, 243-250

[32] Hlaváčová, I.M., Geryk, V., 2016. Abrasives for water-jet cutting of high-strength and thick hard materials. International Journal of Advanced Manufacturing Technology, doi: 10.1007/s00170-016-9462-y

[33] Wang, J.M., Gao, N., Gong, W.J., 2010. Abrasive waterjet machining simulation by SPH method. International Journal of Advanced Manufacturing Technology, 50, 227-234

[34] Kumar, N., Shukla, M. 2012. Finite element analysis of multi-particle impact on erosion in abrasive water jet machining of titanium alloy. J Comput Appl Math, 236, 4600-4610

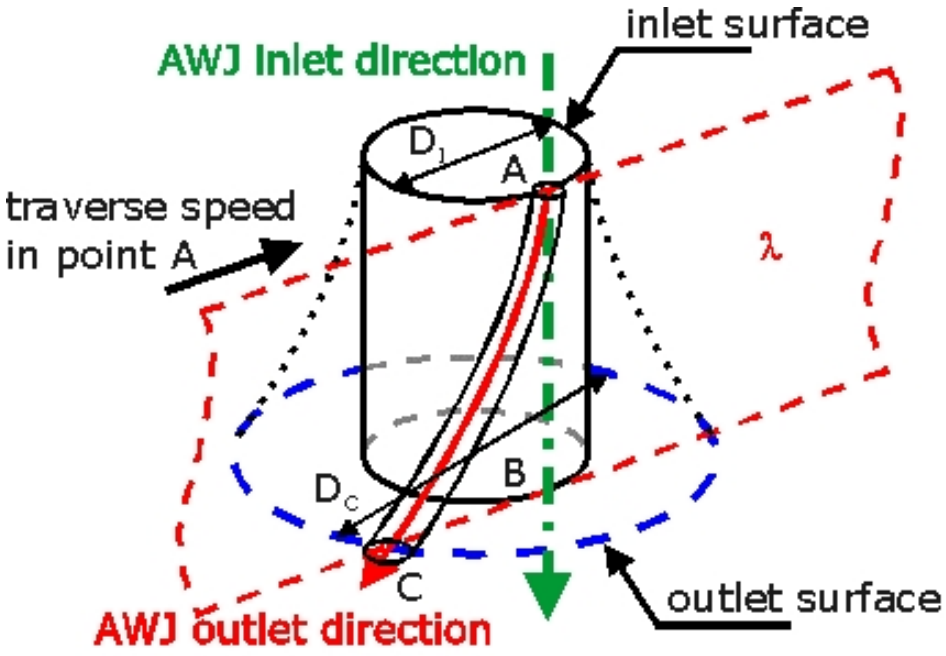
AWJ inlet direction
inlet surface
traverse speed
in point A
D_I
A
λ
B
D_C
C
AWJ outlet direction
outlet surface

a)

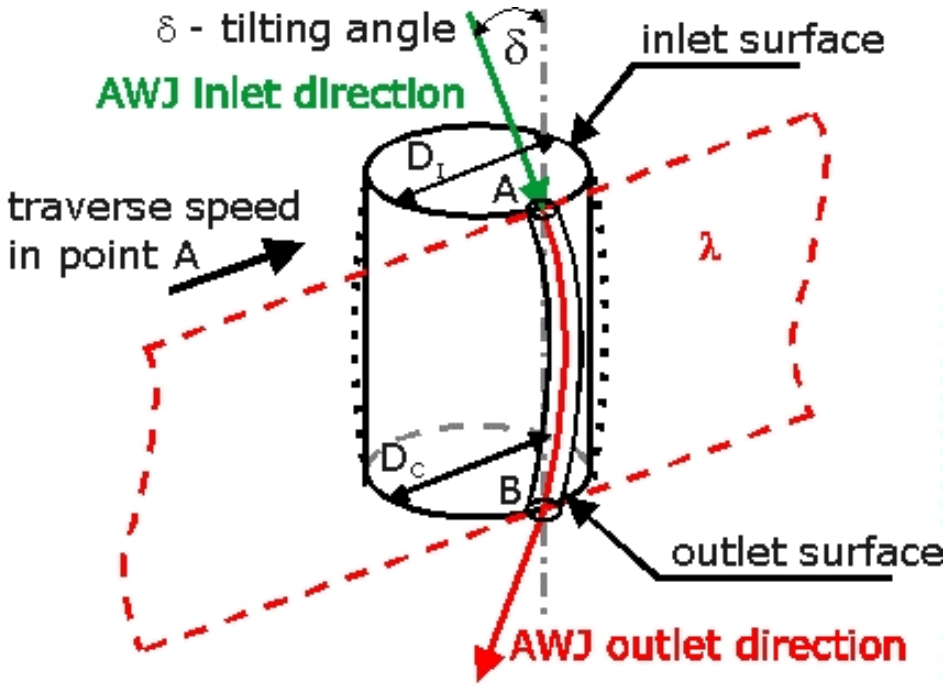
δ - tilting angle
δ
AWJ inlet direction
inlet surface
traverse speed
in point A
D_I
A
λ
D_C
B
outlet surface
AWJ outlet direction

b)

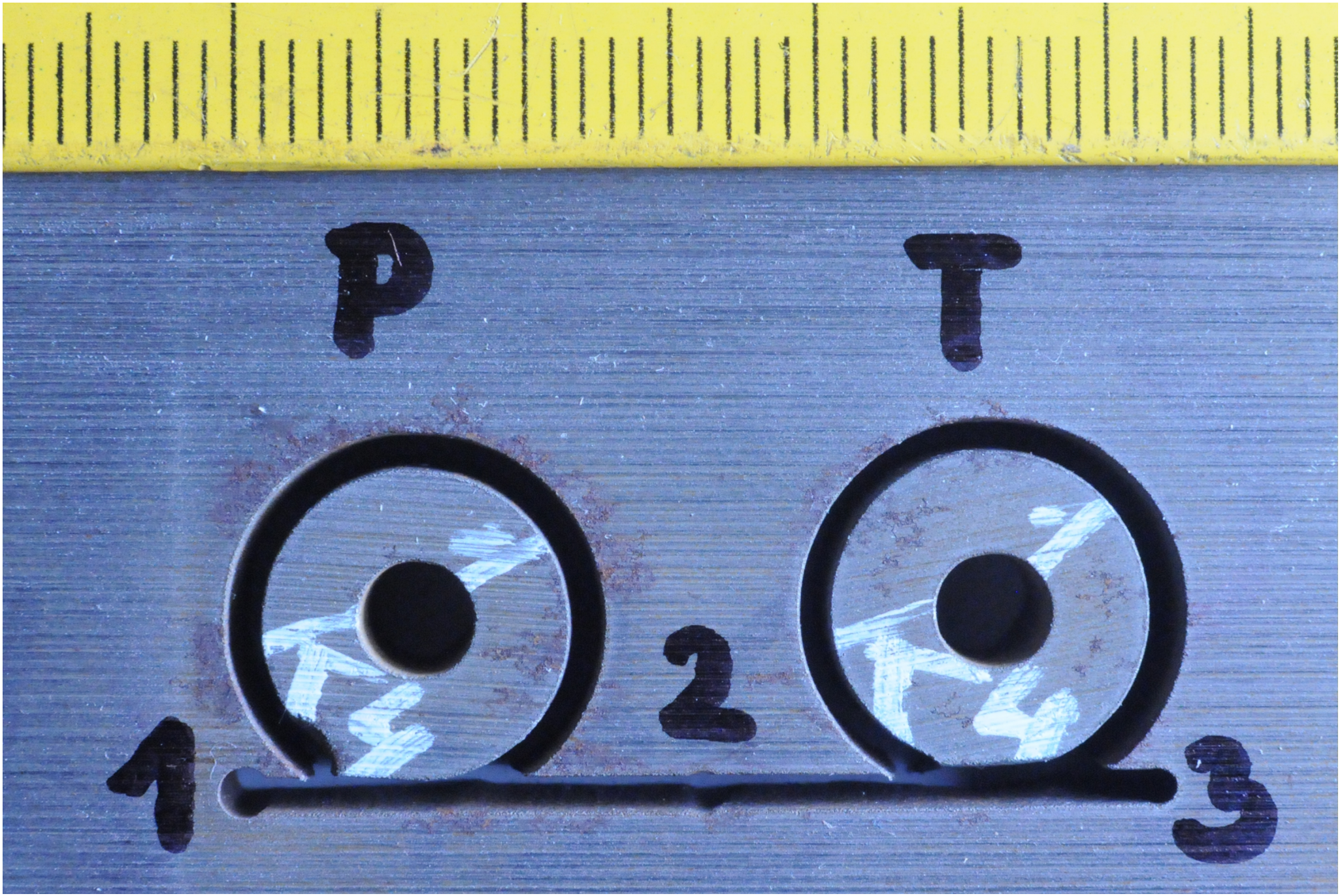
P
T
1
2
3

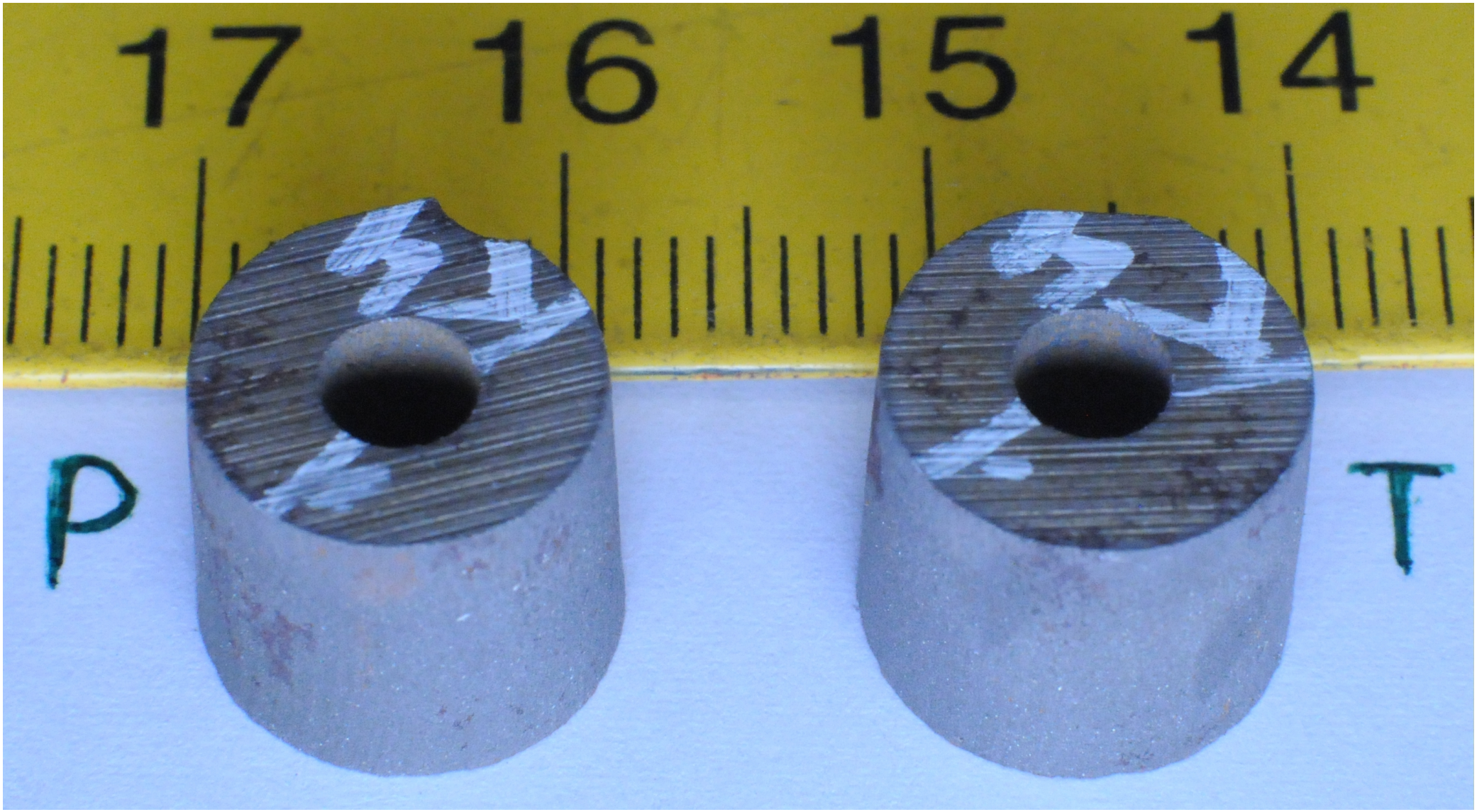
17
16
15
14
P
T

a)
b)

A
7
15
16
17
18


A
NON-TILTED TOP


A
NON-TILTED BOTTOM


B
TILTED TOP


B
TILTED BOTTOM

Tab. 1. Values of pre-set parameters of cutting

Variable (unit)	Ostrava (laboratory)	Milano (machine 1)	Milano (machine 2)
Pressure in pump (MPa)	380	350	350
Water jet diameter (mm)	0.254	0.254	0.330
Focusing tube diameter (mm)	1.02	1.02	1.02
Focusing tube length (mm)	76	76	76
Abrasive mass flow (g/min)	250	300	300
Mean abrasive grain size*) (mm)	0.25	0.25	0.25
Abrasive type**)	AG	AG	AG
Stand-off distance (mm)	2	3	3

*) Measurements of AG garnet 80 mesh was performed in certified Laboratory of Powdery Materials at the VŠB – Technical University of Ostrava on the machine Mastersizer 2000 and confirmed on the Fritsch Analysette 22 MicroTec plus.

**) Abrasive type is almandine Australian garnet (AG)

Tab. 2. Ostrava – perpendicular cuts: Theory and experiment. Steel plate thicknesses *H*, limit traverse speed v_{Plim}, traverse speed v_{P20} calculated for declination angle 20°, theoretical inlet D_{It} and outlet D_{Ot} diameters, experimental inlet D_{Ie} and outlet D_{Oe} diameters, percentage differences ΔD_I and ΔD_O of the average theoretical and experimental values determined for the inlet and outlet diameters.

Material type	H	v_{Plim}	v_{P20}	D_{It} *)	D_{Ie}	D_{Ot}	D_{Oe}	ΔD_I	ΔD_O
WNR norm (DIN norm)	mm	mm/min	mm/min	mm	mm	mm	mm	%	%
1.057 (St 52-3)	10	250	146	8.98	8.96	9.41	9.45	0.22	0.42
1.0503 (C 45)	10	200	116	8.96	9.00	9.52	9.63	0.44	1.14
1.7131 (16 MnCr 5)	10	220	128	8.96	8.92	9.42	9.64	0.45	2.28
1.7225 (42 CrMo 4)	10	180	105	8.96	8.97	9.48	9.64	0.11	1.66
1.4541 (X6 CrNiTi 18 10)	10	200	116	8.96	8.98	9.39	9.36	0.22	0.32
1.2436 (X210 CrW 12)	10	160	93	8.94	8.92	9.64	9.82	0.22	1.83
1.0038 (RSt 37-2)	10	300	175	8.97	8.98	9.50	9.60	0.11	1.04
1.0038 (RSt 37-2)	15	200	116	8.96	8.99	9.62	9.87	0.33	2.53
1.0038 (RSt 37-2)	20	140	82	8.96	8.98	9.98	10.22	0.22	2.35

*) Theoretical inlet diameter is calculated from the circle diameter set on the cutting machine and the diameter of the abrasive water jet calculated from the formula for jet divergence considering stand-off distance measured on machine.

Tab. 3. Milano – cutting on machine 1, first set of samples: Inlet D_I and outlet D_O diameters of "columns" measured on samples prepared at the identical speed v_{P20} intended (calculated) for non-tilted jets producing declination angle 20° and tilted jets with 10° eliminating distortion effects caused by trailback. The percentage differences between the inlet and the outlet column bases are compared for non-tilted ΔD_{N20} and tilted ΔD_{T20} jets.

			non-tilted		tilted		difference	
Material type	H	v_{P20}	D_I	D_O	D_I	D_O	ΔD_{N20}	ΔD_{T20}
WNR norm (DIN norm)	mm	mm/min	mm	mm	mm	mm	%	%
1.057 (St 52-3)	10	146	8.77	9.53	9.14	9.76	8.7	6.8
1.0503 (C 45)	10	116	8.80	9.50	9.13	9.57	7.9	4.8
1.7131 (16 MnCr 5)	10	128	8.81	9.56	9.16	9.79	8.6	6.9
1.7225 (42 CrMo 4)	10	105	8.79	9.40	9.08	9.59	6.9	5.6
1.4541 (X6 CrNiTi 18 10)	10	116	8.80	9.43	9.03	9.52	7.2	5.5
1.2436 (X210 CrW 12)	10	93	8.80	9.51	9.08	9.61	8.1	5.9
1.0038 (RSt 37-2)	10	175	8.87	9.68	9.10	9.70	8.7	4.2
1.0038 (RSt 37-2)	15	116	8.83	10.12	9.02	9.77	13.6	5.9
1.0038 (RSt 37-2)	20	82	8.84	10.58	9.10	10.12	17.9	9.6

Tab. 4. Milano – cutting on machine 1, second set of samples: "Column" samples of stainless and alloyed steels made by non-tilted and tilted jets from 20 mm thick plates: the pre-set traverse speed was 60 mm/min, the inlet D_I and the outlet D_O diameters were measured and the respective percentage differences for non-tilted ΔD_N and tilted ΔD_T jets were determined.

			non-tilted		tilted		difference	
Material type	H	v_{P20}	D_I	D_O	D_I	D_O	ΔD_N	ΔD_T
WNR norm (DIN norm)	mm	mm/min	mm	mm	mm	mm	%	%
1.4034 (X46 Cr 13)	20	60	8.69	11.85	8.95	10.31	30.8	14.1
1.4404 (X2 CrNiMo 17 13 2)	20	60	8.68	11.10	8.93	10.20	24.5	13.2
1.4541 (X6 CrNiTi 18 10)	20	60	8.64	10.92	8.92	10.21	23.4	13.5
1.4713 (X10 CrAl 7)	20	60	8.70	11.20	8.95	9.95	25.1	10.6
1.4762 (X10 CrAl 24)	20	60	8.70	11.30	8.87	10.20	26.0	14.0
1.4828 (X15 CrNiSi 20 12)	20	60	8.64	10.97	8.84	10.24	23.8	14.7
1.4845 (X12 CrNi 25 21)	20	60	8.69	11.09	8.88	11.10	24.2	12.8

Tab. 5. Milano – cutting on machine 2, third set of samples: Inlet D_I and outlet D_O diameters of "columns" measured on samples prepared at the identical speed v_{P20} intended for non-tilted jets producing declination angle 20° and tilted jets with 10° inclination eliminating distortion effects caused by the trailback. The focuser centreline diameter to cut the column base was set to 12 mm (no jet radius offset considered). The percentage differences between the inlet and the outlet column bases are compared for non-tilted ΔD_{N20} and tilted ΔD_{T20} jets.

			non-tilted		tilted		difference	
Material type	H	v_{P20}	D_I	D_O	D_I	D_O	ΔD_{N20}	ΔD_{T20}
WNR norm (DIN norm)	mm	mm/min	mm	mm	mm	mm	%	%
1.057 (St 52-3)	10	193	10.76	11.38	11.18	11.58	5.7	3.6
1.0503 (C 45)	10	153	10.82	11.48	11.13	11.60	6.1	4.2
1.7131 (16 MnCr 5)	10	169	10.82	11.43	11.22	11.59	5.7	3.4
1.7225 (42 CrMo 4)	10	139	10.82	11.39	11.21	11.56	5.3	3.1
1.4541 (X6 CrNiTi 18 10)	10	153	10.82	11.41	11.22	11.58	5.5	3.3
1.2436 (X210 CrW 12)	10	123	10.82	11.50	11.17	11.59	6.3	3.8
3.2315 (AlMgSi1Mn)	10	577	10.75	11.36	11.16	11.51	5.7	3.2
3.1325 (AlCu4MgSi)	10	585	10.78	11.43	11.13	11.54	6.0	3.6
3.4345 (AlZn5Mg3Cu)	10	553	10.85	11.41	11.19	11.53	5.2	3.0
2.0060 (E-Cu57)	10	292	10.90	11.42	11.23	11.51	4.8	2.5
HARDOX500 PLATE	10	103	10.81	11.28	11.18	11.54	4.3	3.2
2.0402 (CuZn40Pb2)	10	290	10.79	11.32	11.20	11.51	4.9	2.8
1.0038 (RSt 37-2)	10	186	10.77	11.37	11.11	11.52	5.6	3.7

Tab. 6. Ostrava – experiments with rotating sample: The fourth set of results was carried out using special device (Fig. 2): inlet D_I and outlet D_O diameters of "columns" are reported. Identical speed v_{P20} applied produces an outlet declination angle of 20° for non-tilted jet and eliminates distortion effects caused by trailback with a 10° jet tilting. The percentage differences between the inlet and the outlet column bases are compared (ΔD_{N20} for non-tilted, ΔD_{T20} for tilted).

			non-tilted		tilted		difference	
Material type	H	v_{P20}	D_I	D_O	D_I	D_O	ΔD_{N20}	ΔD_{T20}
WNR norm (DIN norm)	mm	mm/min	mm	mm	mm	mm	%	%
1.057 (St 52-3)	10	146	8.95	9.95	9.33	9.73	10.6	4.2
1.0503 (C 45)	10	116	8.96	9.88	9.33	9.66	9.8	3.5
1.7131 (16 MnCr 5)	10	128	8.95	9.98	9.32	9.73	10.8	4.3
1.7225 (42 CrMo 4)	10	105	8.95	9.75	9.32	9.63	8.6	3.4
1.4541 (X6 CrNiTi 18 10)	10	116	8.94	9.77	9.31	9.62	8.8	3.2
1.2436 (X210 CrW 12)	10	93	8.95	9.82	9.34	9.66	9.3	3.5
HARDOX 500 PLATE	10	79	8.96	9.63	9.32	9.61	7.1	3.1

Tab. 7. Ostrava – theoretical determination of deformation parameters for non-tilted jet: Trailback, taper and total deformation results calculated by the presented theory and percentage differences of total calculated results from experimental ones presented in Table 6 (left column - inlet diameter, right column - outlet diameter).

				deformation					
Material type	H	v_{P20}	D_I	trailback	taper	D_{OB}	D_O	differences	
WNR norm (DIN norm)	mm	mm/min	mm	mm	mm	mm	mm	%	
1.057 (St 52-3)	10	146	8.96	1.45	0.35	9.54	9.89	0.05	0.60
1.0503 (C 45)	10	116	8.96	1.46	0.36	9.54	9.90	0.00	0.20
1.7131 (16 MnCr 5)	10	128	8.96	1.48	0.36	9.56	9.92	0.12	0.56
1.7225 (42 CrMo 4)	10	105	8.96	1.47	0.36	9.56	9.92	0.16	1.71
1.4541 (X6 CrNiTi 18 10)	10	116	8.96	1.47	0.36	9.55	9.92	0.19	1.49
1.2436 (X210 CrW 12)	10	93	8.96	1.45	0.36	9.54	9.90	0.13	0.85
HARDOX 500 PLATE	10	79	8.96	1.45	0.35	9.54	9.89	0.00	2.68

Tab. 8. Ostrava – theoretical determination of deformation parameters for tilted jet: Trailback, taper and the total compensation results calculated by the presented theory for tilting angle 10° and percentage differences of total calculated results from the experimental ones presented in Table 6 (left column - inlet diameter, right column - outlet diameter). Column D_{OB} is removed because $D_{OB} = D_I$ due to supposed compensation.

				compensation				
Material type	H	v_{P20}	D_I	trailback	taper	D_O	differences	
WNR norm (DIN norm)	mm	mm/min	mm	mm	mm	mm	%	
1.057 (St 52-3)	10	146	9.33	± 0	0.35	9.68	0.01	0.48
1.0503 (C 45)	10	116	9.30	± 0	0.36	9.66	0.28	0.06
1.7131 (16 MnCr 5)	10	128	9.29	± 0	0.36	9.65	0.36	0.84
1.7225 (42 CrMo 4)	10	105	9.30	± 0	0.36	9.66	0.22	0.24
1.4541 (X6 CrNiTi 18 10)	10	116	9.28	± 0	0.36	9.64	0.32	0.25
1.2436 (X210 CrW 12)	10	93	9.31	± 0	0.36	9.67	0.29	0.03
HARDOX 500 PLATE	10	79	9.33	± 0	0.35	9.68	0.14	0.74